Communication

Direct Observation of Growth Defects in Zeolite Beta

Paul A. Wright, Wuzong Zhou, Joaquin Prez-Pariente, and Mar Arranz

J. Am. Chem. Soc., **2005**, 127 (2), 494-495• DOI: 10.1021/ja043948s • Publication Date (Web): 22 December 2004

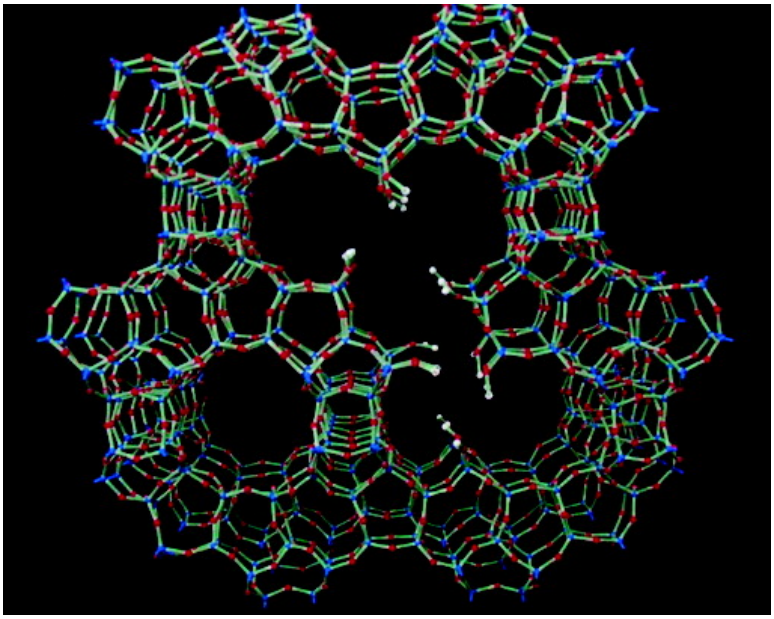

J|A|C|S
COMMUNICATIONS

Published on Web 12/22/2004

Direct Observation of Growth Defects in Zeolite Beta

Paul A. Wright,*,† Wuzong Zhou,*,† Joaquin Pérez-Pariente,‡ and Mar Arranz‡

School of Chemistry, University of St. Andrews, Purdie Building, North Haugh, St. Andrews, Fife KY16 9ST, U.K., and Instituto de Catalisis y Petroleoquimica, CSIC, 28049 Cantoblanco, Madrid, Spain

Received October 5, 2004; E-mail: paw2@st-andrews.ac.uk (P.A.W.); wzhou@st-andrews.ac.uk (W.Z.)

Zeolite beta is one of the most useful high silica zeolites, its interconnected large pore network and strong acidity giving it special catalytic properties. The elucidation of its structure solved a longstanding problem in zeolite crystallography.[1−3] Beta is highly disordered, made up of a random intergrowth of two end-member structures, polytypes A and B of Figure 1, defined by the mode of stacking of complex silicate chain units. Each chain unit is stacked at right angles to chains in the layer below and parallel to other chain units in the same layer. Large pore channels, delimited by 12-MR pores, run parallel to and between adjacent chain units. If two different stacking directions were to occur within the same layer, the frameworks of the two stacking variants would be unable to connect at the boundary. This was taken to explain the observed crystal morphology and also the anomalously large number of defect silanols reported for zeolite beta samples.[2] No direct observation of intracrystalline defects of this sort has been reported, however. Electron microscopy is the most powerful technique for elucidating defect structures;[4] here, we show HRTEM evidence for such defects, shedding light on the crystallization mechanism of zeolite beta and its physical properties.

A sample of pure silica beta was prepared via the fluoride route, according to published procedures,[5] using dimethyldibenzylammonium as template. XRD confirmed the bulk material as beta; SEM showed truncated tetragonal bipyramidal crystals 30 μm long with some amorphous silica. HRTEM was performed using a JEOL JEM-2011 electron microscope operating at 200 kV, with a point resolution of 0.19 nm. The sample is electron beam sensitive, so the microscopic conditions were pretuned and orientation of the crystal was adjusted at low magnification until a principal zone axis was found. Images were recorded at 600 000× using a Gatan 794 CCD camera at very low beam brightness.

HRTEM (Figure 2) reveals the disordered stacking sequence of layers (and 12-membered ring pores) characteristic of zeolite beta. Beta is made up of layers of chain units stacked perpendicular to those of the layer below, a regular distance (a) apart, so that each one is translated by $\pm a/3$ relative to the unit below. There is therefore a family of possible end-members with different stacking sequences,[6] including polytypes A (chain stacking vectors $+a/3$; $-a/3$; $+a/3$, etc.) and B (stacking $+a/3$; $+a/3$, ... along the related direction). The projections (along a common direction relative to the layers of the two polytypes, i.e., [100] for polytype A) are shown in Figure 1. Projections do not distinguish between polytypes which have different stacking vectors for the chain units running parallel to the plane of the paper. It is similarly not possible from TEM images to determine the direction of stacking perpendicular to the page. However, the image (Figure 2) does reveal nanodomains ordered in two dimensions. The microstructure observed here is similar to that of typical samples of beta[1,2] or its natural counterpart, disordered tschernichite,[7] with a structure related to end-members

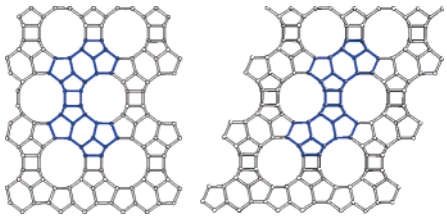

Figure 1. Beta polytypes A (tetragonal, $P4_122$, left) and B (monoclinic $C2/c$, right). Selected units in consecutively stacked layers are shown in blue.

A and B. Figure 2a shows regions in which the stacking vector (equal to $^1/_3$ of the in-layer repeat) is in the same direction for seven, eight and nine successive layers, at least in projection. There are also smaller regions involving five layers where the projection of the stacking vector alternates regularly (as it does in polytype A). Closer inspection also reveals defects that result from adjacent parts of the same layer being related by opposite stacking vectors to a common layer below. This is most easily seen from the different stacking of the large pores (the large white areas in the image). For the case where the displacements are in opposite directions, the layers are observed to come back into registry after three added layers (Figure 2c). The structure of such defects can be modeled in more detail by starting from a layer typical of the beta structure and then adding building units with the two different stacking orientations next to each other. The stacking direction perpendicular to the plane of the paper for this defect is assumed to be in the same direction for the two domains over this region. This is likely since short range order is common. The next layer cannot be completed, but continued growth of the two regions with the same two vectors does enable the subsequent layer to overgrow (Figures 2d and 3). Growth onto this layer can then take place with either stacking direction.

The interrupted structure results in Q3 silicons (Si(−OSi−)$_3$OH) lining the defect as shown in the model, which were made using a kit with atomic centers of appropriate geometry (Figure 3). Silanol hydroxyls are known to be a marked feature of beta materials.[2] The model shows remarkable agreement with the image. The predicted arrangement of two pores, double and one-and-a-half times as large as the usual large 12-MR pore, is mirrored. Furthermore, careful inspection of the secondary detail is also in agreement. Fourier averaging of a "perfect" region of the structure gives the image in Figure 2b. At this resolution, it is possible to resolve, in addition to the large pores, the areas of low projected electron density that result from six-, five-, and even four-membered rings. Building units made up from four 5-MRs and one 6-MR in projection (outlined in Figure 1) are observed to stack in the same orientation. Although the image of the defects (Figure 2c) is noisier (their irregular distribution prevents Fourier averaging), it is possible to make out the orientation of building units of this type. Going through each defect along a layer, we observe that the orientation

† University of St. Andrews.
‡ Instituto de Catalisis y Petroleoquimica.

10.1021/ja043948s CCC: $30.25

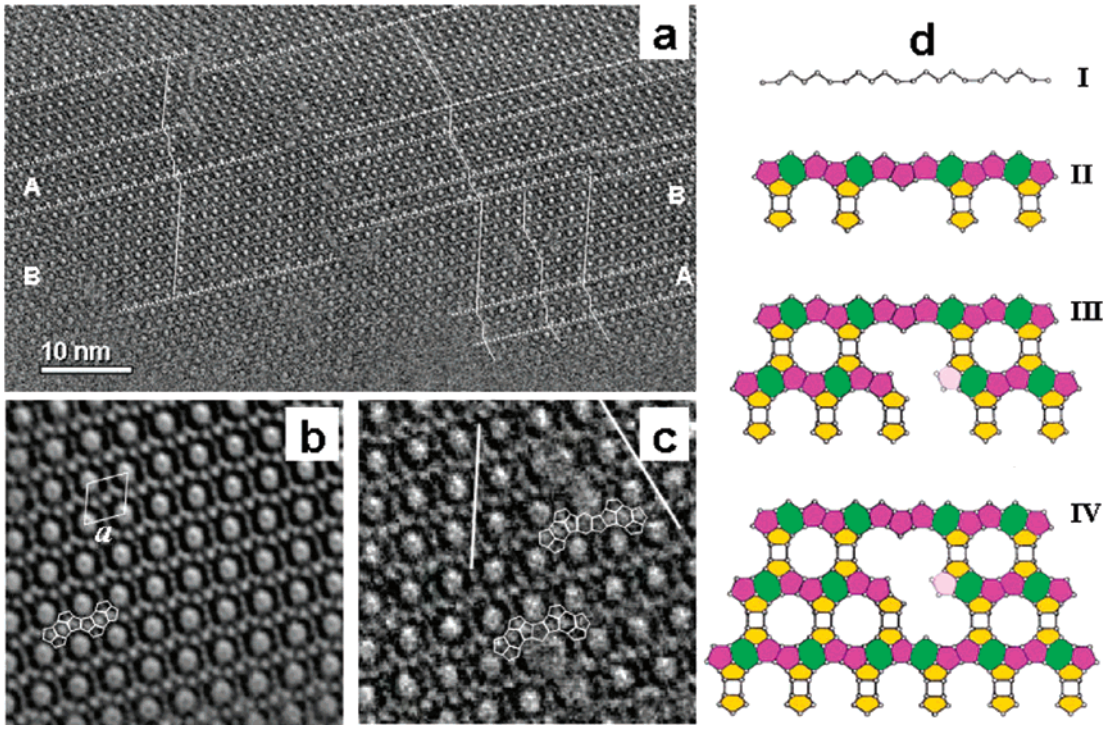

Figure 2. (a) HRTEM of an edge of a beta crystallite, annotated to show the stacking directions in different parts. Nanodomains related to polytypes A and B are indicated. Defects are visible in the center of the image, where domains with different stacking directions meet. (b) Fourier-averaged image of a domain of type B, with structural units outlined. (c) Image of two double pore defects, showing different stacking directions and outlining secondary structural details on either side of the defects. (d) Suggested crystal growth sequence, indicating how the defects form and how the building units adopt different orientations at the defect (similar subunits are colored in similar colors; only the pale unit at the core of the defect cannot unambiguously be identified in the image).

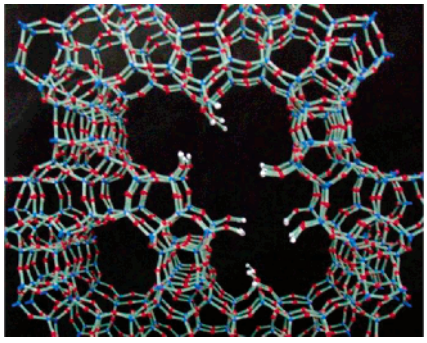

Figure 3. Model of the observed defects, obtained by stacking in the two ways onto a single layer and continuing to the third similar layer. The cages indicated in light pink in Figure 2d may or may not be complete. Here they are not, whereas they are in the model shown in the graphical abstract.

of these units reverses. The exact nature of the core of the defect remains unclear, even at such high resolution; models are possible with or without [5^4•4^3] cages building out into the pores. Computation studies may resolve the issue.[8] The linear defects (perpendicular to the plane of projection) run through the structure. The two larger pores are partly partitioned by hydroxyls, but the space within the pore system is enlarged, particularly at the intersections of the defects with channels running perpendicular.

Observation of these defects casts light on two intriguing aspects of the synthesis and growth of zeolite beta. First, they are consistent with a layer-by-layer growth mechanism for beta, where growth may nucleate at different parts of the same layer with different stacking vectors. Such a growth mechanism is shown schematically in Figure 2d, indicating how the defects could heal. A similar mechanism has been suggested for the double defects observed in ETS-10 by Anderson et al.[9] Jones et al.[10] have shown that functionalized siloxanes can be incorporated within the pores of beta during synthesis, without loss of order, giving shape-selective, organic-functionalized microporous catalysts. It is tempting to speculate that organic groups could be incorporated at defects similar to those described here. Finally, the defects suggest a way to include well-defined mesoporosity within a zeolite if nucleation rates can be controlled by changing synthesis conditions.

Acknowledgment. CICYT (MAT 2003-07769.C02-02) and the Spanish Ministries of Science (M.A.) are thanked for funding. Dr. T. Blasco (ITQ, Valencia) is thanked for the NMR spectra.

Supporting Information Available: XRD and ^{29}Si MAS NMR. This material is available free of charge via the Internet at http://pubs.acs.org.

References

(1) Treacy, M. M. J.; Newsam, J. M. *Nature* **1988**, *332*, 249.
(2) Newsam, J. M.; Treacy, M. M. J.; Koetsier, W. T.; de Gruyter, C. B. *Proc. R. Soc. A* **1988**, *420*, 375−405.
(3) Higgins, J. B.; LaPierre, R. B.; Schlenker, J. L.; Rohrman, A. C.; Wood, J. D.; Kerr, G. T. *Zeolites* **1988**, *8*, 446.
(4) Thomas, J. M.; Terasaki, O.; Gai, P. L.; Zhou, W.; Gonzalez-Calbet, J. *Acc. Chem. Res.* **2001**, *34*, 583.
(5) Arranz, M.; Garcia, R.; Pérez-Pariente, J. In *Proceeding of the 14th International Zeolite Conference*, South Africa, 2004; p 256.
(6) Gies, H.; van Koningsveld, H. *Catalogue of Disorder in Zeolite Frameworks* (http://www.iza-structure.org/database/).
(7) Szostak, R.; Pan, M.; Lillerud, K. P. *J. Phys. Chem.* **1995**, *99*, 2104.
(8) Ohsuna, T.; Slater, B.; Gao, F.; Yu, J.; Sakamoto, Y.; Zhu, G.; Terasaki, O.; Vaughan, D. E. W.; Qiu, S.; Catlow, C. R. A. *Chem.—Eur. J.* **2004**, 5031.
(9) Anderson, M. W.; Agger, J. R.; Hanif, N.; Terasaki, O. *Microporous Mater.* **2001**, *48*, 1.
(10) (a) Jones, C. W.; Tsuji, K.; Davis, M. E. *Nature* **1998**, *393*, 52. (b) Jones, C. W.; Tsapatsis, M.; Okubo, T.; Davis, M. E. *Microporous Mater.* **2001**, *42*, 21.

JA043948S